

NJC

Accepted Manuscript



This is an *Accepted Manuscript*, which has been through the Royal Society of Chemistry peer review process and has been accepted for publication.

Accepted Manuscripts are published online shortly after acceptance, before technical editing, formatting and proof reading. Using this free service, authors can make their results available to the community, in citable form, before we publish the edited article. We will replace this *Accepted Manuscript* with the edited and formatted *Advance Article* as soon as it is available.

You can find more information about *Accepted Manuscripts* in the [Information for Authors](#).

Please note that technical editing may introduce minor changes to the text and/or graphics, which may alter content. The journal's standard [Terms & Conditions](#) and the [Ethical guidelines](#) still apply. In no event shall the Royal Society of Chemistry be held responsible for any errors or omissions in this *Accepted Manuscript* or any consequences arising from the use of any information it contains.



NJC

paper

Selective removal of copper with polystyrene-1, 3-diaminourea chelating resin: Synthesis and adsorption studies

C. Shen^a, Y. Chang^a, L. Fang^b, M. Min and C. H. Xiong^{*a}Received 00th January 20xx,
Accepted 00th January 20xx

DOI: 10.1039/x0xx00000x

www.rsc.org

Copper, as a common heavy metal, is harmful to the environment and to people's health. In this study, green chloromethylated polystyrene beads (PS-Cl) 1, 3-diaminourea(DU) which was to adsorb copper ions was synthesized from chloromethylated polystyrene(PS-Cl) and 1, 3-diaminourea(DU). The structure was characterized by FT-IR and elemental analysis. The adsorption properties of the resin for Cu(II) were investigated by batch and column experiments. Batch adsorption results suggested that PS-DU had high adsorption capability for Cu(II) and maximum saturated adsorption capacity was 168.7mg/g at 308K, estimated from the langmuir model. The resin and its metal complexes were studied by TGA, SEM and XPS. Furthermore, the resin can be eluted easily using 2mol/L HCl. PS-DU can not only provide a potential application for selective removal of copper from waste solution, also provide an application in the analysis and detection area.

Introduction

The pollution of water resources due to the indiscriminate disposal of metals has been concerned in the last few decades¹. Copper, as one of the important heavy metals, is released to the aqueous environment from wastewater such as oil refinery, battery manufacturing industries, and chlor-alkal manufacturing². Exposure to copper can destroy the nervous system in humans, especially for the developing nervous system of young children³. Hence, removing copper from aqueous environment to reduce its hazards is a critical task in the perspective of environment and health. So far, several technologies have been developed for the removal of copper containing effluents, such as ion exchange⁴⁻⁵, chemical precipitation⁶, adsorption, electrolytic and electrochemical separation⁷⁻⁸, among which adsorption is regarded as a guaranteed and practical treatment method because of advantages such as they are low cost, ecofriendly, and easy to handle, and they have high enrichment factors, high recovery, and high selectivity for some metal ions⁹⁻¹⁰. A wide range of materials can be used to remove copper from solutions such as chitosan¹¹⁻¹², nanoadsorbent¹³ and porous material¹⁴.

Green macroporous chloromethylated polystyrene beads(PS-Cl) are an ideal polymeric matrix with a stable mechanical property. Active chloro-(Cl) present in polystyrene, which can be transformed

into various new functional groups by special reactions¹⁵⁻²⁰. Resins functionalized with groups containing sulfur or nitrogen were highly efficient in the selective adsorption of metals²¹⁻²².

According to the experiences, combined with spatial effect and electronic effect ligands by quantum chemical calculations, we screened several ligands, and regarded 1, 3-diaminourea(DU) ligands as the final choice on the basis of a large number of experimental. The chelating resin we prepared by grafting 1,3-diaminourea on the polymer compound (macroporous chloromethylated cross-linked polystyrene microspheres), which had an ideal adsorption effect for Cu (II). The synthetic resin was characterized by FT-IR, elemental analysis(EA), TGA and XPS. To further understand the adsorption process, The data of adsorption kinetics, isotherms, and the thermodynamic mechanism were also studied. The resin was supposed to fit in with the environmental protection.

Experimental section

Materials

Macroporous chloromethylated polystyrene beads (PS-Cl for short) with a degree of cross-linking of 8% DVB, a chlorine content of 19.15%, and a specific surface area of 43 m²/g were purchased from the Chemical Factory of Nankai University(China). 1,3-diaminourea(DU) was from Aladdin Industrial Corporation, China. Aqueous solutions of ions at various concentrations were prepared from NiSO₄·6H₂O, HgCl₂, CuCl₂·2H₂O, Zn(NO₃)₂·6H₂O, Cd(NO₃)₂·4H₂O, and Pb(NO₃)₂ and were used as sources for Ni(II), Hg(II), Cu(II), Zn(II), Cd(II) and Pb(II), respectively. All other reagents and solvents were of analytical reagent grade and were used without further purification.

^aDepartment of Applied Chemistry, Zhejiang Gongshang University, No. 149 Jiaogong Road, Hangzhou, 310012, PR, China, E-mail: xiongch@163.com; Tel: +86-0571-88071024-7571

^bState Department of Food Science and Human Nutrition, University of Florida, Bldg 475 Newell Drive, Gainesville, FL 32611, USA

† Electronic Supplementary Information (ESI) available: See DOI: 10.1039/x0xx00000x

Apparatus

IR spectra for the samples were obtained from a Nicolet 380 Fourier transform infrared (FT-IR) spectrometer. X-ray photoelectron spectroscopy (XPS) of the resins were obtained with an ESCALab220i-XL electron spectrometer from VG Scientific using 300W AlK α radiation. The concentrations of metal ions were measured by Inductively Coupled Plasma Optical Emission Spectroscopy (ICP-OES). Thermogravimetric analysis was performed using a Mettler TGA (with a temperature range of 25-800°C, a heating rate of 20°C/min, and an atmosphere of N₂). Scanning electron micrographs for the samples were obtained using a HITACHI S-3000N scanning electron microscope (SEM). C, N and S elements were analyzed by a Vario ELIII Elemental Analyzer. The specific surface area and the mean pore size of the resins were determined on an Autosorb-1 automatic surface area and pore size analyzer. The sample was shaken in a DSHZ-300A temperature constant shaking machine. The water used in the present work was purified using a Mol research analysis type ultrapure water machine. A Mettler Toledo delta 320 pH meter was used for pH measurement. The respective zeta potentials of PS-DU resins were determined by a zeta potential analyzer (Malvern Zetasizer Nano ZS90).

Preparation of PS-DU

The preparation procedure is briefly described as follows: 0.5 g of PS-Cl beads and 300 mL of Dimethyl sulfoxide (DMSO) were added into a 500 mL three-neck round-bottom flask, swelling overnight. Then, 2.11 g of DU (molar ratio of reagent (DU/PS-Cl)=3) and a small amount of metallic sodium used as catalyst were added to the flask. The mixture reacted for 10 h at 85°C under a nitrogen atmosphere. The solid product was carefully washed thoroughly with DMSO and deionized. Subsequently the obtained resin was dried in vacuum at 50°C. The conversion of the functional group of the synthetic resin can be calculated from nitrogen content by the following equations:

$$F_c = \frac{N_c}{14 \times n_c} \times 1000$$

$$X = \frac{F_n \times 1000}{1000 \times F_0 - \Delta m \times F_n \times F_0} \times 100\%$$

where F₀ (mmol of Cl/g) and F_c are the contents of the functional group of polystyrene and the synthesized resin, respectively, X is the functional group conversion (%), Δm is the incremental synthesis reaction resin (g/mol), n_c is the number of nitrogen atoms of ligand molecules, and N_c is the nitrogen content of the synthesized resin (%).

Resin adsorption and desorption experiments

Batch experiments were carried out to investigate the Cu(II) adsorption property on the prepared PS-DU resin by placing 15.0 mg resin in a series of flasks containing 30 mL of the studied metal ions at the desired initial concentration and pH. Then the contents of the flasks were shaken in a flask-shaker at specific temperature for a given time with a speed of 100 rpm. The residual concentration of the studied metal ions in the solution was

determined by ICP. The adsorption capacity (Q, mg/g) and distribution coefficient (D, mL/g) were calculated with the following expression:

$$Q = \frac{C_0 - C_e}{W} V$$

$$D = \frac{C_0 - C_e}{WC_e} V$$

where C₀ is the initial concentration of Cu(II) (mg/mL), C_e is the residual concentration of Cu(II) in solution (mg/mL), V is the solution volume (mL), and W is the resin dry weight (g). The above batch adsorption experiments for the adsorption of Cu(II) by PS-DU in aqueous solutions were performed at different pH values, contact times, initial concentrations of Cu(II) and temperatures. The operating variables studied for the extent of adsorption were pH, contact time, initial concentration and temperature.

Desorption experiments were carried out following the completion of the adsorption experiments. After adsorption experiments, the resins were separated from the aqueous solution by filtration, washed with deionized water, and shaken with different eluent solutions of various concentrations at 298 K for 24 h. After that time the concentration of Cu(II) was similarly analyzed as described above. After each adsorption-desorption cycle, the resin beads were washed and reconditioned for adsorption in the succeeding cycle. The desorption ratio (E) was calculated as follows:

$$E(\%) = \frac{C_d V_d}{(C_0 - C_e) V} \times 100\%$$

where C_d is the concentration of the solutes in the desorption solutions, V_d is the volume of the desorption solution, and C₀, C_e and V are the same as defined above.

Column experiments were carried out in a fixed-bed mini glass column (ϕ 3mm \times 30cm) under the optimum pH 3.5 obtained from the batch experiments at a constant temperature of 298 K, which is close to the environmentally relevant conditions. Then, 100.0 mg PS-DU was presoaked in the column for 24 h before the experiment began. In order to avoid the channeling of the effluent, a certain concentration of Cu(II) solution in a constant flow rate was passed continuously through the stationary bed of sorbent in up-flow mode. The outgoing Cu(II) concentration was determined at different time intervals as described above.

Results and discussion

Characterization of PS-DU

The structures of PS-Cl, DU, and PS-DU were confirmed by FT-IR spectroscopy as shown in **Figure 1**. In general, it is observed that there are significant changes in the IR spectra of PS-Cl resin and PS-DU resin. As compared with the curve of PS-Cl, the characteristic peaks at 1263 and 672 cm⁻¹, which are assigned to CH₂-Cl, disappeared as expected. In the spectra of PS-DU, the characteristics bands of -NH₂ at 3414 and 3176 cm⁻¹ disappeared, whereas a strong and broad characteristic band of secondary amine (N-H) peak at 3403 cm⁻¹ and the antisymmetric stretching vibration band at 3020 cm⁻¹ and symmetric stretching vibration band at 2924 cm⁻¹ of -CH₂ groups appeared, which confirmed that the reaction between the CH₂-Cl and -NH₂ group occurred. Furthermore, the PS-DU resin was characterized by the characteristic peak of C=O at

NJC

1741 cm^{-1} , C-N at 1604 cm^{-1} , and N-H at 1604 cm^{-1} , which is further evidenced that the presence of DU introduced to the modified polymer²³⁻²⁷. The characteristics and elemental analysis of the resin are shown in **Table 1**. The specific surface area and mean pore size are slightly changed after grafting of DU with PS-Cl. The new appearance of N content confirmed the grafting of DU ligands on the surface of the PS-Cl polymer. The functional group capacity of the newly synthetic resin (PS-DU) was 3.22mmol/g obtained from the elementary analysis of N, and the functional group conversion was 50.9%. The potential synthesis routes of PS-DU resin is presented in **Scheme 1**, on the basis of the FT-IR analysis.

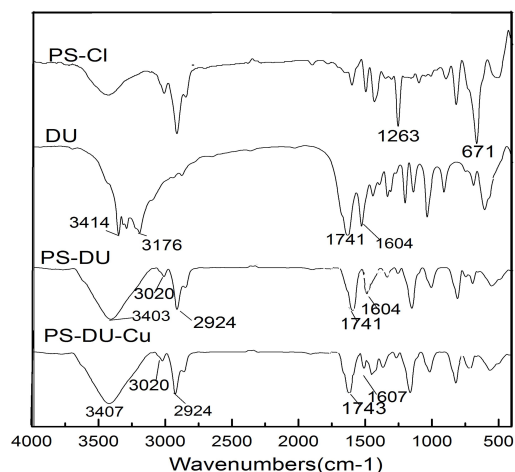


Figure 1 FT-IR spectra of PS-Cl, DU, PS-DU and PS-DU-Cu.

Table 1 Characteristics and elemental analysis data of the resin.

	N content (%)	Functional group content	Functional group conversion (%)	Specific surf.area (m^2/g)	Mean pore size (nm)
PS-Cl				43.0	31.2
PS-DU	19.6	3.22mmol/g	50.9	43.3	31.3

The FT-IR spectra of the Cu(II) adsorbed resin (PS-DU-Cu) was also revealed to find out the adsorption mechanism. In the spectra of PS-DU-Cu, the $\nu_{\text{C=O}}$ and $\nu_{\text{C-N}}$ stretching bands were shifted to lower wavenumbers by 2 cm^{-1} (from 1741 to 1743 cm^{-1}), and 3 cm^{-1} (from 1604 to 1607 cm^{-1}), respectively, which suggested that the oxygen atoms and nitrogen atoms in DU were involved in Cu(II) adsorption. In addition, the -N-H stretching band decreased and shifted slightly (from 3403 to 3407 cm^{-1}), indicating that the secondary amine is also available in the Cu(II) binding process²⁸.

The thermo-gravimetric analysis (TGA) was used to examine the thermal stability of the PS-DU resin before and after adsorption of Cu(II), and the TGA curve obtained as shown in **Figure 2**. The decomposition of PS-Cl had two steps. In the first step, the temperature increased from 25 to 400 $^{\circ}\text{C}$, The weight loss of this step can be attributed to the fracture chloromethyl bond. In the second step, an increase in temperature from 400 to 800 $^{\circ}\text{C}$ was observed, which indicates that the skeleton structure of PS-Cl was broken. DU began to decompose at 200 $^{\circ}\text{C}$ and the decomposition

reached 100% at 500 $^{\circ}\text{C}$. In terms of PS-DU, the slight weight loss before 300 $^{\circ}\text{C}$ may be attributed to the emitted water and volatile materials, a further weight loss from 300 to 400 $^{\circ}\text{C}$, resulting from the decomposition of DU grafted to PS-Cl, after that a sharp weight loss occurred at 400-520 $^{\circ}\text{C}$ with degradation of the chloromethyl chains. Similar to PS-DU, the TGA curve of PS-DU-Cu also included two steps. Compared to the weight loss rate of PS-DU, the weight loss rate of PS-DU-Cu was slightly less than 20 wt% resulting from adsorption of copper on PS-DU²⁹.

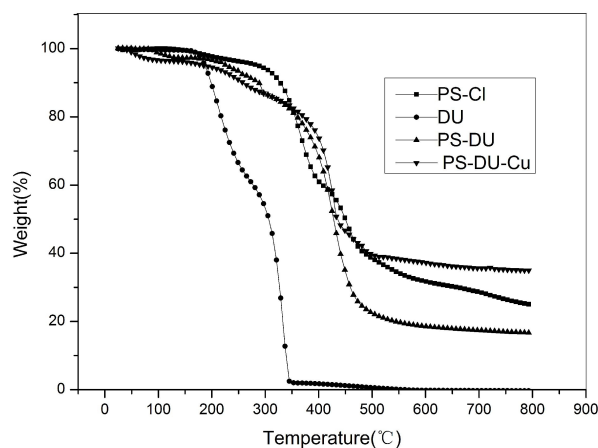
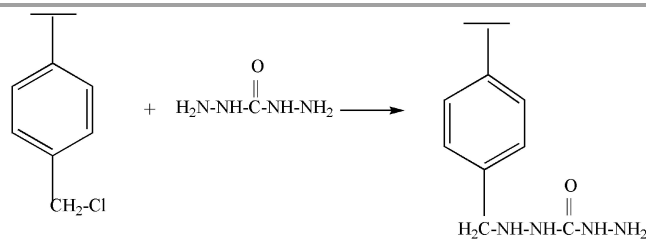


Figure 2 TGA curves of PS-Cl resin, DU, PS-DU resin and PS-DU-Cu resin.



Scheme 1 Synthesis routes for PS-DU.

Effect of pH

The pH of aqueous solution is one of the most important factors for adsorption of metal ions³⁰. The effect of pH on the adsorption behavior of PS-DU resin for Cu(II) was shown in **Figure 3**. It could be seen that adsorption capacity for Cu(II) was highest when pH value was 3.5 in the HAC-NaAc medium and adsorption capacity decreased by either raising or lowering pH. Cu(II) was present in the aqueous solution in the forms of Cu^{2+} , $\text{Cu}(\text{OH})^+$, $\text{Cu}(\text{OH})_2$, $\text{Cu}(\text{OH})_3^-$, $\text{Cu}(\text{OH})_4^{2-}$ ³¹. Since the zeta potentials of the PS-DUs are positive at $\text{pH} < 3.5$ (point of zero charge, pH_{zpc}), the interactions between the adsorption sites on PS-DUs and the copper ions are electrostatically repulsive. As the solution pH increases, the repulsion between adsorbent surface and metal ions becomes weaker, thus enhancing the adsorption capacity. On contrary, at pH above pH_{zpc} , $\text{Cu}(\text{OH})_3^-$ and $\text{Cu}(\text{OH})_4^{2-}$ were the dominant species, -N-H playing the major role in binding activity and PS-DU became deprotonated (-N-),

paper

NJC

which may be electrostatically repulsive between adsorption sites on PS-DU and $\text{Cu}(\text{OH})_3$, $\text{Cu}(\text{OH})_2$. As the solution pH increases, the repulsion between adsorbent surface and metal ions becomes stronger, thus reducing the adsorption capacity. Therefore, when the pH=6, the adsorption capacity of the resin is very small. The adsorption studies at pH>6 were not conducted because of the precipitation of $\text{Cu}(\text{OH})_2$ from the solution.

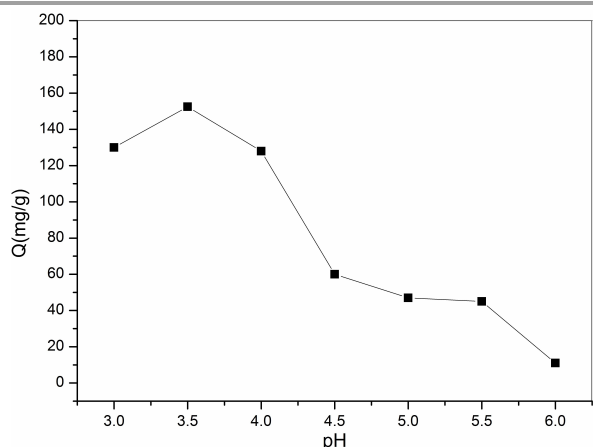


Figure 3 Effect of pH on the adsorption capability of PS-DU for Cu(II) (resin 15.0 mg, initial metal ion concentration = 10.0 mg/30.0 mL, pH3–6, T = 298 K, 100 rpm).

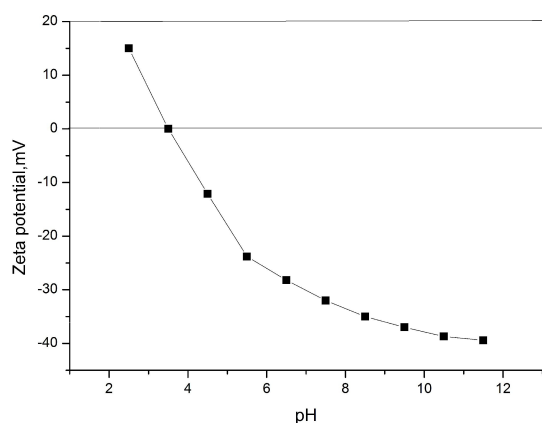


Figure 4 Zeta potentials of PS-DU resin at different pH.

The selective adsorption property was also investigated in a mixed metal solution containing Cu(II), Ni(II), Zn(II), Cd(II), Hg(II), and Pb(II) metal ions in the same pH range. The result were shown **Figure 5**. It suggested that PS-DU has much higher affinity toward Cu(II) than the other metal ions. The highest adsorption capacity for Cu (II) was 149.8mg/g at pH 3.5 in the HAC-NaAc system which shows high selectivity and adsorption capacity for Cu(II)³²⁻³³. The high adsorption capacity and selectivity for Cu(II) result from the different nitrogen groups in the PS-DU that show different affinities to Cu(II) and the Ni(II), Hg(II), Cd(II), Pb(II), and Zn(II) metal ions. The -N-H and -C-N group contributes to the high adsorption capacity toward Cu(II), and the -C=O group contributes to the high selectivity toward Hg(II), because it is a very soft basic and has a superior affinity with Cu(II) ions.

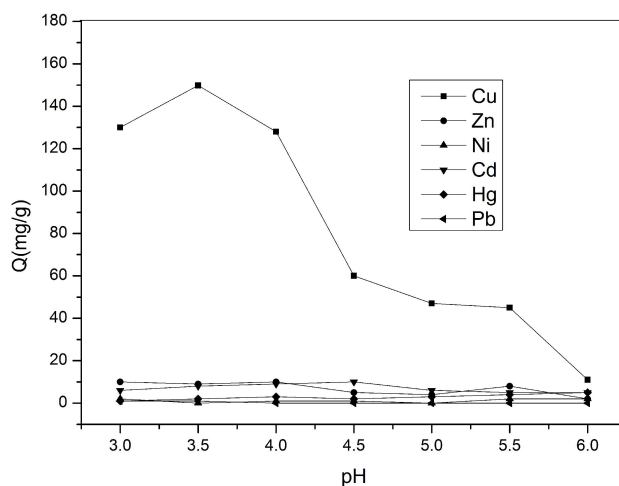


Figure 5 The capacity of PS-DU resin in different pH values.

Kinetic study of copper removal

Figure 6 shows the influence of contact time on adsorption of Cu(II) onto PS-DU at various temperatures ranging from 288K to 308K. It can be clearly seen that a rapid adsorption of Cu(II) by PS-DU occurs at different temperatures within 10 hours, and then adsorption increased slowly until the equilibrium state reached at 30h. Meanwhile the equilibrium adsorption increased within the range of reaction temperatures(288-308K), which was close to the great swelling of the resin and increased diffusion of metal ions into the resin at a higher temperatures. This indicates that the mechanism associated with Cu(II) adsorption onto PS-DU involves a temperature-dependent process. The adsorption kinetics of Cu(II) on PS-DU is investigated with the help of three kinetic models, namely The pseudo-first-order³⁴, The pseudo-second-order³⁵ and the Elovich models³⁶.

The pseudo-first-order kinetic model is given as:

$$\ln(Q_e - Q_t) = \ln Q_1 - \frac{k_1}{2.303} t$$

The pseudo-second-order equation is expressed as:

$$\frac{t}{Q_t} = \frac{1}{k_2 Q_2^2} + \frac{t}{Q_2}$$

The Elovich equation can be described as:

$$Q_t = \frac{1}{\beta} \ln(\alpha\beta) + \frac{1}{\beta} \ln t$$

In Eqs, Q_t (mg/g) is the adsorption capacity at time t , Q_e (mg/g) is the adsorption capacity at equilibrium. k_1 (min^{-1}) and k_2 ($\text{mg}/(\text{g min})$) are the adsorption rate constants of pseudo-first-order, and pseudo-second-order isotherms. α and β are Elovich parameters, which represent the initial adsorption rate ($\text{mg}/(\text{g min})$) and the desorption constant (g/mg), respectively.

NJC

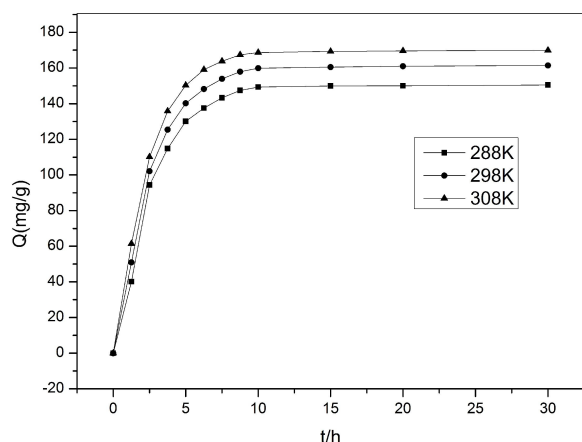


Figure 6 Adsorption kinetics and capacity Q at different times and different temperatures (resin 15.0 mg, $[Cu^{2+}]_0 = 10.0$ mg/30.0 mL, pH 3.5, 100 rpm).

The correlation coefficient R^2_2 for the pseudo-second-order equation was better than the correlation coefficient R^2_1 for the Lagergren first-order equation. Moreover, the experimental-calculated capacity of the pseudo-second-order model produces alternatives, as observed in **Table 2**. Therefore, the adsorption behavior of Cu(II) on PS-DU resin successfully explained by a pseudo-second-order mechanism, which means the chemical adsorption is the rate-controlling step.

Table 2 Kinetic parameters for Cu(II) adsorption by PS-DU.

	Q_e (mg/g)	K_1 (min^{-1}) $\times 10^3$	Q_1 (mg/g)	R^2
Pseudo-first-order				
288K	136.6 ± 3.2	1.02 ± 0.02	116.6 ± 3.1	0.973 ± 0.001
288K	141.0 ± 3.9	1.15 ± 0.03	121.1 ± 3.5	0.977 ± 0.003
308K	145.6 ± 4.3	1.23 ± 0.04	139.6 ± 3.6	0.981 ± 0.002
	Q_e (mg/g)	K_2 ($\text{g}/(\text{mg min}) \times 10^3$)	Q_2 (mg/g)	R^2
Pseudo-second-order				
288K	136.6 ± 3.2	1.42 ± 0.02	154.2 ± 3.6	0.993 ± 0.002
288K	141.0 ± 3.9	1.87 ± 0.04	159.6 ± 3.9	0.989 ± 0.003
308K	145.6 ± 4.3	1.79 ± 0.03	163.2 ± 4.3	0.991 ± 0.002
	Q_e (mg/g)	A (mg/g.min)	β (g/mg) $\times 10^2$	R^2
Elovich				
288K	136.6 ± 3.2	2.62 ± 0.02	0.92 ± 0.02	0.938 ± 0.002
288K	141.0 ± 3.9	3.81 ± 0.04	1.01 ± 0.04	0.941 ± 0.003
308K	145.6 ± 4.3	5.79 ± 0.03	1.04 ± 0.03	0.966 ± 0.002

Isotherm of adsorption

In order to gain a better understanding of the mechanism, three

models are utilized to fit the sorption data. The Langmuir isotherm³⁷ is represented by the following equation:

$$\frac{C_e}{Q_e} = \frac{C_e}{Q_0} + \frac{1}{Q_0 b}$$

where C_e (mg/L) is the equilibrium concentration of metal ions remaining in solution, Q_e (mg/g) is the amount of metal ions adsorbed per weight unit of sorbent after equilibrium, Q_0 (mg/g) is the maximum sorption capacity of metal ions, and b (L/mg) is a constant that relates to the heat of sorption.

The Freundlich model³⁸ is represented by the following equation:

$$\ln Q_e = \ln K_f + \frac{1}{n} \ln C_e$$

where Q_e , C_e is defined as above, $1/n$ is an empirical parameter involves the adsorption intensity, which varies with the heterogeneity of material, and K_f is roughly an indicator of the adsorption capacity.

The Redlich-Peterson³⁹ model is represented as follows:

$$Q_e = \frac{K_{rp} C_e}{1 + \alpha_{rp} C_e^\beta}$$

where K_{rp} and α_{rp} are Redlich-Peterson constants, and β is basically in the range of 0 and 1. The D-R equation⁴⁰ has the general expression as follows:

$$\ln Q_e = \ln Q_m - \beta \varepsilon^2$$

where Q_e is the amount of adsorbed Hg(II) per unit adsorbent (mg/g), Q_m is the calculated adsorption capacity, β is activity coefficient pertinent to mean adsorption energy, and ε is Polanyi potential, which can be calculated through:

$$\varepsilon = RT \ln(1 + 1/C_e)$$

Isotherm parameters for Cu(II) adsorption by PS-DU showed in **table 3**. Mean adsorption energy, E (kJ/mol), is very useful to determine the mechanisms of adsorption process, which can be expressed as the following equation:

$$E = 1/\sqrt{2\beta}$$

The magnitude of E is useful to estimate the type of sorption reaction. The E value in the range of 1-8 kJ/mol indicates physical adsorption; the value between 8 and 16 kJ/mol signifies an ion-exchange process; its value in the range of 20-40 kJ/mol is indicative of chemisorption. The values of E (kJ/mol) (288 K, 8.4; 298 K, 9.91; 308 K, 10.32) were founded to be above 8 kJ/mol, indicating that the Cu(II) adsorption on PS-DU is a chemical process. The Langmuir model was best fitted to the experiment results over the other isotherms comparing the three theoretical models to the experimental data, demonstrating that the adsorption of Cu(II) on PS-DU is of a monolayer type where interactions between adsorbed molecules are negligible.

Table 3 Isotherm parameters for Cu(II) adsorption by PS-DU.

	Q_0	b	R^2
Langmuir			
288K	157.2 ± 4.9	12.4 ± 1.5	0.993 ± 0.004
298K	163.4 ± 5.2	14.5 ± 1.4	0.996 ± 0.003
308K	168.7 ± 5.9	15.7 ± 1.7	0.997 ± 0.004
	$1/n$	K_f (mg/g)/(mg/ml) ^{1/n}	R^2

Freundlich				
Temperature (K)	K_{rp}	α_{rp}	β	R^2
288K		0.29 ± 0.02	179.2 ± 5.1	0.927 ± 0.007
298K		0.27 ± 0.01	181.1 ± 5.4	0.901 ± 0.009
308K		0.25 ± 0.02	186.5 ± 5.3	0.871 ± 0.006
Redlich-Peterson				
Temperature (K)	K_{rp}	α_{rp}	β	R^2
288K	8.79 ± 0.56	0.0498 ± 0.0017	0.875 ± 0.047	0.901 ± 0.004
298K	9.27 ± 0.42	0.0525 ± 0.0023	0.901 ± 0.039	0.900 ± 0.008
308K	10.79 ± 0.63	0.0573 ± 0.0041	0.941 ± 0.049	0.871 ± 0.006
		β (mol ² /J ²). 10 ⁹	Q_m	R^2
D-R				
Temperature (K)	K_{rp}	α_{rp}	β	R^2
288K		4.8 ± 0.26	159.7 ± 3.5	0.961 ± 0.003
298K		4.1 ± 0.23	166.2 ± 3.9	0.912 ± 0.002
308K		3.6 ± 0.49	171.4 ± 4.7	0.874 ± 0.004

Thermodynamic parameters

The temperature of this adsorption experiment was varied to study the thermodynamic feasibility of the adsorption process. Adsorption of 10mg/30 mL Cu(II) was performed (with 15.0 mg adsorbent dose) at 288, 298, and 308K. Solution pH was maintained at 3.5. Thermodynamic parameters such as the Gibbs free energy (ΔG), enthalpy (ΔH), and entropy (ΔS) for the adsorption process can be determined by using following equations⁴¹:

$$\log D = -\frac{\Delta H}{2.303RT} + \frac{\Delta S}{2.303R}$$

where R is the universal gas constant D is the distribution coefficient and T is the absolute temperature. From which (the enthalpy variation) and ΔS (the entropy Variation) are deduced from the slope and intercept of the line, respectively. And the free energy variation ΔG , was calculated from:

$$\Delta G = \Delta H - T\Delta S$$

The thermodynamic parameters of the sorption of Cu(II) were calculated and the results are given in **Table 4**. The positive value of ΔH confirms the endothermic nature of adsorption which is also supported by the increase in value of Cu(II) uptake of the adsorbent with the rise in temperature, As a result, process is significant and rate controlling. The negative value of all ΔG indicates the feasibility of the process and spontaneous nature of metal ion adsorption onto PS-DU adsorbents. The magnitude of ΔG decreases with increasing temperature indicating that adsorption is favorable at higher temperatures. Enhancement of adsorption capacity of PS-DU at higher temperatures may be attributed to the greater swelling of the resin and increased diffusion of metal ions into the resin. In addition, the values of ΔS are found to be positive due to the exchange of the metal ions with more mobile ions present on the exchange, which would cause increase in the entropy, during the adsorption process⁴²⁻⁴³.

Table 4 The thermodynamic parameters for Cu(II) adsorption by PS-DU.

ΔH (KJ/mol)	ΔG (KJ/mol)			ΔS (J/(Kmol))
	T=288K			
	T=298K	T=308K		
15.1	-13.9	-16.1	-18.4	114.2

Dynamic Adsorption and Desorption

The fixed bed column operation allows more efficient utilization of the adsorptive capacity than the batch process. One of the main tools used in the investigation of the efficiency in adsorption columns is the breakthrough analysis⁴⁴. Total sorption capacity of metal ion (Q) in the column for a given feed concentration and flow rate is calculated by

$$Q = \int_0^V \frac{(C_0 - C_e)}{m} dV$$

where C_0 and C_e are metal ion concentrations in the influent and effluent (mg/mL), respectively, m is the total weight of the sorbent loaded in the column, and V is the volume of metal solution passed through the column (mL). The capacity value Q was obtained by graphical integration as 151.4mg/g. Successful design of a column sorption process requires prediction of the concentration-time profile or breakthrough curve for the effluent. Traditionally, the Thomas model is used to fulfill the purpose. The model has the following form:

$$\frac{C_e}{C_0} = \frac{1}{1 + \exp[K_T(Q_m - C_0)/\theta]}$$

where K_T is the Thomas rate constant (mL/(min mg)), h is the volumetric flow rate (mL/min), and m is the mass of the resin (g). The linearized form of the Thomas model is as follows⁴⁵:

$$\ln\left(\frac{C_0}{C_e} - 1\right) = \frac{K_T Q_m}{\theta} - \frac{K_T C_0}{\theta} V$$

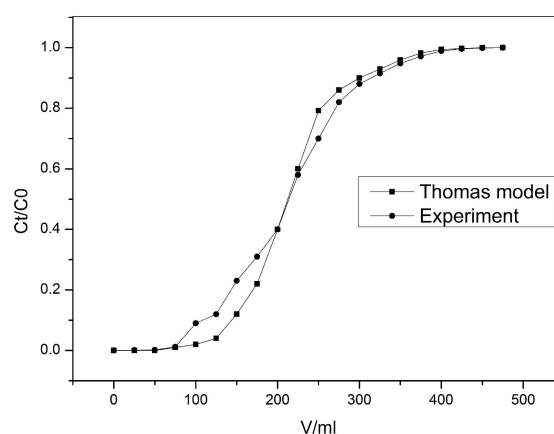


Figure 7 Experimental and predicted breakthrough curves using the Thomas model for Cu(II) adsorption by PS-DU resin, at 298 K, pH 3.5, 100 rpm.

The kinetics coefficient K_T and the adsorption capacity Q of the column can be determined from a plot of $\ln[(C_0/C_e) - 1]$ versus t at a

NJC

certain flow rate. The Thomas equation coefficient for Cu(II) adsorption was $K_T = 1.63 \times 10^{-2} \text{ mL}/(\text{mg}/\text{min})$ and $Q = 137.1 \text{ mg}/\text{g}$. The theoretical predictions based on the model parameters were compared with the observed data as shown in **Figure 7**. Considering the high R^2 value (0.9983) and the good agreement of the calculated Q with the experimental data, the Thomas model can be applied to design and simulate column adsorption process. With respect to the dynamic desorption of Cu(II) from PS-DU, the 2.0 mol/L HCl eluent was employed. The desorption curve was plotted with the effluent concentration (C_e) versus elution volume (V) from the column at a flow rate of 0.1 mL/min. As shown in **Figure 8**, a sharp increase of Cu(II) concentration was observed and 50 mL 2.0 mol/L HCl eluent solution provided effectiveness of the desorption of Cu(II) from PS-DU, after which further desorption is negligible.

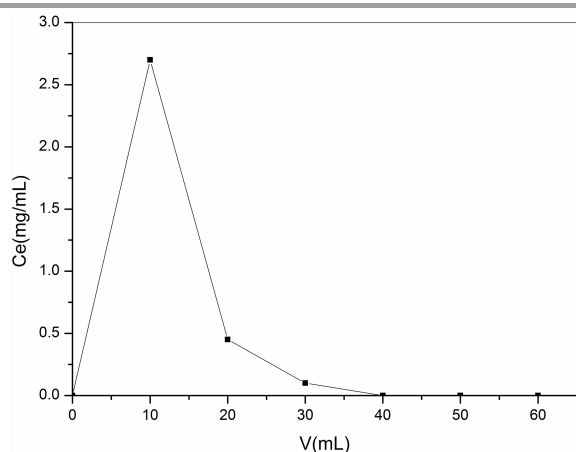


Figure 8 Dynamic desorption curve flow rate $\frac{1}{4}$ 0.1 mL min⁻¹.

Desorption and Regeneration studies

From practical perspective, repeated availability is a crucial factor for an advanced adsorbent. Such adsorbent has higher adsorption capability as well as better desorption property which will reduce the overall cost for the adsorbent. Cu(II) saturated PS-DU were eluted with 30 mL HCl in various concentrations (0.5–4.0 mol/L) under 100 rpm at 298 K for 24 h. The desorption data shows that the adsorbed Cu(II) can be completely desorbed by 2 mol/L HCl solution with a desorption ratio of 100%. In order to show the reusability of the adsorbent, the adsorption-desorption cycle of metal ions was repeated five times using the same beads. The results of the five adsorption-desorption cycles are shown in **Table 5**, indicating that the adsorption capacity was barely affected during the repeated adsorption-desorption operations and the adsorption capacity was maintained at 91.2% after five cycles. These results suggest that PS-DU could be repeatedly used in the enhanced removal of Cu(II) from waste solution.

Data on the adsorption capacity and desorption ratio of Cu(II) by the recent reported adsorbents^{11–14,46–50} were listed in **Table 6**. Though some materials exhibited a higher adsorption capacity of Cu(II), the PS-DU with a good overall property (a high adsorption capacity and a 100% desorption ratio) used for Cu(II) removal is still very attractive. Furthermore, PS-DU can be reused many times, and has a high specific selective adsorptivity compared to the recent reported adsorbents.

Table 5 Reusing the PS-DU for the adsorption of Cu(II).

Cu ²⁺	Adsorption capacity(mg/g)				
	First time	Second time	Third time	Fourth time	Fifth time
	145.9	141.1	137.9	133.2	131.6

Table 6 Adsorption capacities of different adsorbents.

adsorbent	Adsorption capacities(mg/g)	Desorption ratio	Refs.
polystyrene supported chitosan	99.8	84	11
Cross-linking chitosans	112	-	12
anatase nanoparticles	23.74	-	13
Carboxylic acid functionalized porous material	37.5	97.6	14
Amino modification of biochar	16.11	97	46
Graphene oxide (GO)-cds composite	112.5	90	47
Ordered mesoporous carbon(OMC)	56.62	-	48
Polyaniline graft chitosan beads (PGCB)	100	97.1	49
Mesoporous silica material	62	-	50
PS-DU	168.7	100	This work

SEM and XPS analysis

The morphologies and surface composition of PS-DU before and after Cu(II) adsorption were characterized by SEM and showed in **figure 9**. Obviously, the smooth surface of PS-DU became coarser after Cu(II) was adsorbed, which showed that copper was loaded on the surface of the resin.

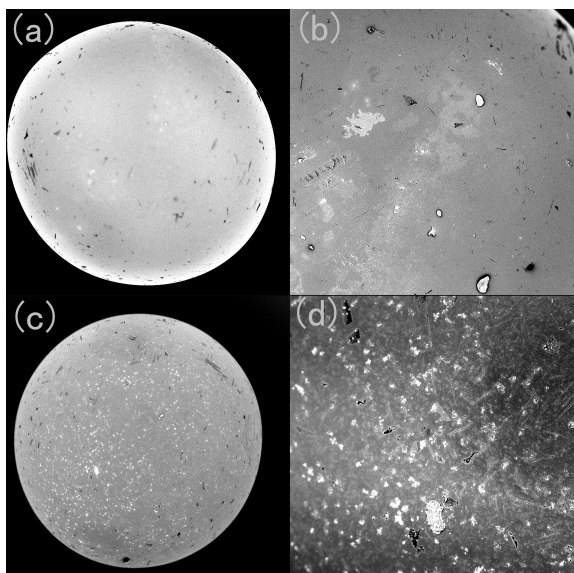


Figure 9 SEM images of PS-DU resin and PS-DU-Cu resin. (a) PS-DU resin at a magnification of 250; (b) PS-DU resin at a magnification of 1000; (c) PS-DU-Cu resin at a magnification of 250; (d) PS-DU-Cu resin at a magnification of 1000.

XPS analysis was performed to investigate the molecular level information of copper adsorption on the PS-DU resin. **Figure 10** showed XPS spectra of PS-DU, Cu(II) loaded PS-DU and CuCl₂. Before copper adsorption, the N1s binding energy located at 400.2 eV is composed of a signal, which belongs to the nitrogen in –C–N– in the resin. After gold adsorption, the N1s band was shifted to 402.4 eV, due to the formation of bonds between the nitrogen and the copper. In **table 7**, Atomic content of O 1s increased dramatically from 13.64% to 24.82%, which displays a significant intensity decrease and shift toward higher binding energy after copper adsorption, indicating that a complex between copper and oxygen occurred. The Cu(II) 2p spectrum is typical for CuCl₂, indicating the adsorption of copper in the resin.

Table 7 Atomic Content(%) of the PS-DU before and after Adsorption.

	C 1s	N 1s	O 1s	Cu 2p
PS-DU	82.05	4.31	13.64	
PS-DU-Cu	60.32	6.13	24.82	8.73

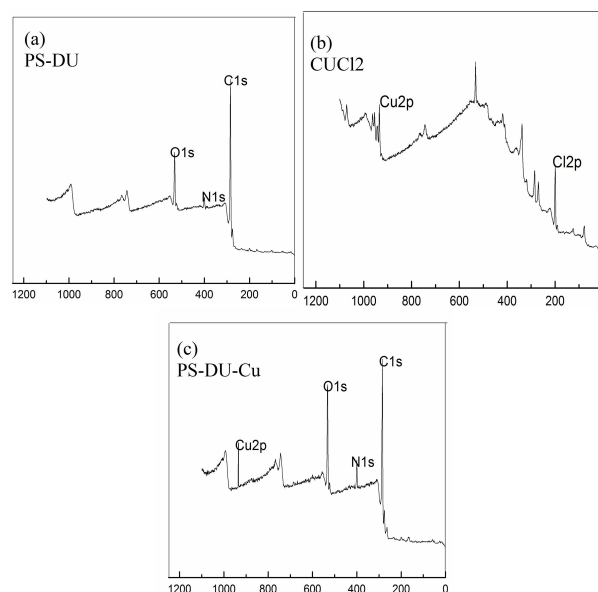


Figure 10 XPS spectra of PS-DU, Cu(II) loaded PS-DU and CuCl₂, (a) PS-DU, (b) CuCl₂, (c) PS-DU-Cu.

Conclusions

In this paper, a new composite chelating resin containing N donor atoms has been synthesized. FT-IR and elemental results indicate that the immobilization of DU onto PS-Cl was accomplished. Batch adsorption results showed that the resin possess an excellent selective adsorption ability of Cu(II) in the mixed metal solutions containing Hg(II), Ni(II), Cu(II), Cd(II), Pb(II), and Zn(II) metal ions. The adsorption process follows pseudo-second-order model, suggesting that chemisorption is the rate-controlling step. The well fits to the Langmuir isotherm indicates that the monolayer adsorption is dominant. The adsorption process is endothermic and spontaneous at ambient higher temperature. Meanwhile, the Thomas model is applied to experimental data obtained from dynamic studies performed on a fixed column to predict the breakthrough curves and to determine the column kinetic parameters. Complete desorption of Cu(II) was achieved by using 2 mol/L HCl solution, and the regenerated adsorbents could be reused with little loss of adsorption capacity. In conclusion, PS-DU resin may satisfactorily be considered as an alternative material for separation applications and recovery of Cu(II) from aqueous solutions. Furthermore, it also offers promising applied in the area of analysis and detection.

Acknowledgements

The work is supported by the National Natural Science Foundation of China (No. 21276235), Ph.D. Programs Foundation of Ministry of Education of China (No. 20133326110006), Funds of Zhejiang Provincial Key Lab. of Industrial Textile Materials & Manufacturing Tech.

NJC

Notes and references

- 1 J. C. Benassi, R. Laus, R. Geremias, P. L. Lima, and C. T. Menezes, *Arch. Environ. Con. Tox.*, 2006, 51, 633.
- 2 C. H. Xiong, Y. L. Li, G. T. Wang, L. Fang, S. G. Zhou and C. P. Yao, *Chem. Eng. J.*, 2015, 259, 257.
- 3 G. Aragay, J. Pons and A. Merkoci, *Chem. Rev.*, 2011, 111, 3433.
- 4 M. K. Doula, *Water Res.*, 2009, 43, 3659.
- 5 M. K. Doula, and A. Dimirkou, *J. Hazard. Mater.*, 2008, 151, 738.
- 6 M. M. Matlock, B. S. Howerton, and D. A. Atwood, *Water Res.*, 2002, 36, 475.
- 7 I. Heidmann, and W. Calmano, *J Hazard Mater.*, 2008, 152, 934.
- 8 L. C. Ajjabi, and L. Chouba, *J. Environ.*, 2009, 90, 3485.
- 9 H. Zhang, B. Dai, X. Wang, W. Li, Y. Han, J. Gu and J. Zhang, *Green Chem.*, 2013, 15, 829.
- 10 R. S. Azarudeen, M. A. Riswan-Ahamed, and A. R. Burkanudeen, *Desalination.*, 2011, 90, 268.
- 11 W. Jiang, X. Chen, B. Pan, Q. Zhang, L. Teng, and Y. Chen, *J. Hazard. Mater.*, 2014, 276, 295.
- 12 Y. S. Petrovaa, A. V. Pestov, M. K. Usoltsevaa and L. K. Neudachina, *J. Hazard. Mater.*, 2015, 299, 696.
- 13 Z. Özlem, K. Ataklı, and Y. Yürüm, *Chem. Eng. J.*, 2013, 225, 625.
- 14 J. Han, Z. J. Du, W. Zou, H. Q. Li and C. Zhang, *Chem. Eng. J.*, 2015, 262, 571.
- 15 C. H. Xiong and C. P. Yao, *Chem. Eng. J.*, 2009, 155, 844.
- 16 C. H. Xiong, X. Y. Chen, and C. P. Yao, *Curr. Org. Chem.*, 2012, 16, 1942.
- 17 H. Yang, X. Han, G. Li and Y. Wang, *Green Chem.*, 2009, 11, 1184.
- 18 R. J. Qu, C. H. Wang, C. M. Sun, C. N. Ji, G. X. Cheng, X. Q. Wang, and G. Xu, *J. Appl. Polym. Sci.*, 2004, 92, 1646.
- 19 C. M. Sun, R. J. Qu, C. H. Wang, C. N. Ji and G. X. Cheng, *J. Appl. Sci.*, 2005, 95, 890.
- 20 N. Charef, Z. Benmaamar, L. Arrar, A. Baghiani, R. M. Zalloum, and M. S. Mubarak, *Solvent Extr. Ion. Exc.*, 2012, 30, 101.
- 21 F. E. Beamish, *Talanta.*, 1967, 14, 991.
- 22 E. M. Moyers and J. S. Fritz, *Anal. Chem.*, 1976, 48, 1117.
- 23 M. Conte, C. J. Davies, D. J. Morgan, T. E. Davies, A. F. Carley, P. Johnston and G. J. Hutchings, *Catal. Sci. Technol.*, 2013, 3, 128.
- 24 M. Yildirim, and A. Kayal, *Synth. Met.*, 2012, 162, 436.
- 25 C. H. Xiong, Q. Jia, X. Y. Chen, G. T. Wang, and C. P. Yao, *Ind. Eng. Chem. Res.*, 2013, 52, 4978.
- 26 P. Samadhiya, R. Sharma, S. K. Srivastava, and S. D. Srivastava, *Chin. J. Chem.*, 2011, 29, 1001.
- 27 S. Saydam, and E. Yilmaz, *Acta. A.*, 2006, 63, 506.
- 28 L. G. Han, Y. P. Tao, H. Q. Liang, and Z. J. Liu, *Chin. J. Light Scattering.*, 2010, 22, 6.
- 29 G. R. Kiani, H. Sheikhoie, and N. Arsalani, *Desalination.*, 2011, 269, 266.
- 30 H. Chen, G. Dai, J. Zhao, A. Zhong, J. Wu, and H. Yan, *J. Hazard. Mater.*, 2010, 177, 228.
- 31 G. Zhao, H. Zhang, Q. Fan, X. Ren, J. Li, Y. Chen, and X. Wang, *J. Hazard. Mater.*, 2010, 173, 661.
- 32 E. Guibal, *Sep. Purif. Technol.*, 2004, 38, 43.
- 33 J. Wang, B. L. Deng, H. Chen, X. R. Wang and Z. Zheng, *Environ. Sci. Technol.*, 2009, 43, 5223.
- 34 Y. S. Ho, and G. McKay, *Process Saf. Environ. Prot.*, 1998, 76, 332.
- 35 Y. S. Ho, *Water Res.*, 2003, 37, 2323.
- 36 K. Aparecida, G. Gusmao, L. V. A. Gurgel, T. M. S. Melo, and F. Gil, *Dyes Pigments.*, 2012, 92, 967.
- 37 I. Langmuir, *J. Am. Chem. Soc.*, 1918, 40, 1361.
- 38 H. M. F. Freundlich, *Phys. Chem.*, 1906, 57, 385.
- 39 S. J. Allen, G. McKay, and J. F. Porter, *J. Colloid Interface. Sci.*, 2004, 280, 322.
- 40 M. M. Dubinin, and L. V. Radushkevich, *Chem. Zentralbl.*, 1947, 1, 875.
- 41 L. C. Zheng, Z. Dang, X. Y. Yi, and H. Zhang, *J. Hazard. Mater.*, 2010, 176, 650.
- 42 A. Sari, M. Tuzen, M. Citak and D. M. Soylak, *J. Hazard. Mater.*, 2007, 149, 283.
- 43 A. A. Shaikh, C. S. Othman, A. Hamouz, and N. M. Hassan, *J. Hazard. Mater.*, 2013, 47, 248.
- 44 N. H. Mthombeni, L. Mpenyana-Monyatsi, M. S. Onyango, and M. N. Momba, *J. Hazard. Mater.*, 2012, 217, 133.
- 45 T. Mathialagan and T. Viraraghavan, *J. Hazard. Mater.*, 2002, 94, 291.
- 46 G. X. Yang, and H. Jiang. *Water Res.*, 2014, 48, 396.
- 47 T. S. Jiang, W. P. Liu, Y. Mao, L. Zhang, J. L. Chen, M. Gong, H. B. Zhao, L. M. Dai, S. Zhang and Q. Zhang, *Chem. Eng. J.*, 2015, 259, 603.
- 48 C. C. Huang, and J. C. He, *Chem. Eng. J.*, 2013, 221, 469.
- 49 E. Igberase, P. Osifo, and A. Ofomaja, *J. Envi. Chem. Eng.*, 2014, 1, 362.
- 50 X. D. Zhao, L. Z. Song, Z. H. Zhang, R. Wang, and J. Fu, *J. Mol. Struct.*, 2013, 986, 68.